

CHROM. 17,199

## SAMPLING AND FLOW EFFECTS IN SEDIMENTATION FIELD FLOW FRACTIONATION\*

C. H. DILKS, Jr., W. W. YAU and J. J. KIRKLAND\*

*E. I. Du Pont de Nemours & Company, Central Research and Development Department, Experimental Station, Wilmington, DE 19898 (U.S.A.)*

(Received August 31st, 1984)

---

### SUMMARY

Transparent model channels for sedimentation field flow fractionation (SFFF) were devised so that sample-introduction patterns and primary flow characteristics could be visualized. If a sample is injected at a point beyond the channel inlet, just where the full width of the channel is realized, less band broadening and more accurate retention results are obtained, as compared with injection of particles with the entering mobile phase stream via a valve loop. However, this injection method was found to be less convenient. Valve-loop injection can be used with good results, providing that loops of relatively small volume are utilized, and the sample is slowly swept from the loop into the channel inlet with the mobile phase. Expected retention of particles in SFFF experiments was obtained only with optimum injection techniques designed to place the sample as a sharp pulse at the channel inlet.

---

### INTRODUCTION

Sedimentation field flow fractionation (SFFF) is a versatile method that can be used to separate dispersed particulates of about 0.005–2  $\mu\text{m}$  diameter, or dissolved macromolecules in the molecular-weight range of about  $10^6$ – $10^{12}$  (see refs. 1–5). Separation occurs in a channel formed between two closely spaced concentric surfaces, rotated in a centrifuge. The imposed centrifugal force causes sample species to be forced towards the inner or outer wall; particles denser than the mobile phase are forced towards the outer wall. Diffusion causes particles to establish a specific layer thickness near the wall, as a function of mass. A liquid phase flowing through the channel assumes a characteristic parabolic velocity flow profile, so that particles near the wall reside in regions of slower flow. Small particles, or lower-molecular-weight materials that are not influenced by the external force field, are engaged by all flow streams within the channel and elute first, at one channel volume. Retained sample components then are carried by the mobile phase at a smaller average velocity in the channel to a detector at the outlet; smaller particles elute first, followed by compo-

---

\* Presented in part at the *Eastern Analytical Symposium, November 18–20, 1983.*

nents of increasing mass. The resulting fractogram provides quantitative information on the mass of the sample constituents. More detailed descriptions of the workings and quantitative relationships involved in SFFF are described elsewhere<sup>1,3-5</sup>.

Sample retention and resultant mass measurements can be strongly influenced by the manner in which the sample is introduced into the SFFF channel. In the work of Giddings *et al.*<sup>3</sup>, sample injection was made directly into the separating channel by microsyringe with the rotor at rest. However, with large sample injection volumes, earlier-than-theoretical elution of the peaks can occur, because a portion of the channel is occupied initially by the sample. Direct syringe injection of the sample also is inconvenient when the time-delayed exponential force field decay technique (TDE-SFFF) is used, because the rotor is spinning at its highest speed at the beginning of the experiment<sup>5-7</sup>.

If the sample is injected with an applied force field (centrifuge running), the effective volume occupied by the sample at the channel inlet is reduced, relative to sample injection with no force field, since particles are tightly held at the channel inlet by the force field. If this retaining force field is large, sample components are forced into a narrow band at the channel inlet during sampling. This effect decreases the potential for band broadening and minimizes potential retention errors because a much reduced portion of the channel volume is used by the injected sample. Thus, with high initial force fields, large sample volumes can be injected without seriously affecting retention; sample relaxation times also are minimized.

Previously it has been shown that samples may be introduced from the loop of a microsampling valve with good results<sup>4</sup>. This approach is especially useful when the TDE-SFFF technique is used. In the present work systematic experiments were conducted to determine the sweep volume required to displace loop contents and transport the sample into the channel with a minimum of deleterious effects. Sample relaxation was also studied in which the particles were allowed to sediment to equilibrium within the channel with the mobile phase not flowing prior to fractionation under a force field.

Recently, the effects of channel breadth (span) and the design of the channel entrance and exit configurations were studied by others to elucidate the mechanism of zone broadening due to channel configuration<sup>8</sup>. Model channels were constructed to study this effect, and small solutes were utilized at zero field strength. In the present work, techniques were devised by which sample-introduction patterns and primary flow characteristics of model SFFF channels could be visualized. The purpose of our approach was to develop information to permit the optimization of sample-injection techniques so that accurate SFFF retention would result over a wide range of operational variables. A special feature of this study was that particulates rather than small molecules were used to determine flow characteristics. In a second aspect of this research, the sample-injection technique was studied with the aid of transparent channels. In addition, the effect of valve-loop sweep volume and particle relaxation time were investigated, particularly in TDE-SFFF operation.

## EXPERIMENTAL

### *Apparatus*

Special transparent model channels and appropriate accessory equipment were

assembled for the visibilization studies. These are described in detail in appropriate sections below. The SFFF apparatus used in the sampling studies of retention and band broadening was previously described<sup>2,4,5</sup>. A MINC microcomputer (Digital Equipment Corporation, Maynard, MA, U.S.A.) was interfaced with the SFFF apparatus to control several operational parameters and to make the particle-size calculations as previously described<sup>5</sup>. Basic theory for TDE-SFFF operation has been reported earlier<sup>6</sup>.

### *Reagents*

Polystyrene latex standard samples were obtained from Dow Diagnostics (Dow Chemical, Midland, MI, U.S.A.). Aerosol-OT surfactant used to prepare the mobile phase was obtained from Fisher Scientific (Pittsburgh, PA, U.S.A.).

## RESULTS AND DISCUSSION

### *Channel flow patterns*

The primary objective of this part of the study was to develop and demonstrate a technique by which sample-introduction patterns and primary flow characteristics in an SFFF channel could be visibilized. The general experimental approach was to use the same size and concentration of particles that are of interest in actual SFFF analyses. Preliminary studies involving the possible benefits of various injection systems were also performed.

Initial flow-profile studies were carried out in a stationary transparent model channel that was 6 in. long and 1 in. wide (span). These experiments permitted the visibilization of sampling and channel-inlet flow characteristics. The channel bottom consisted of an  $8 \times 4 \times 1/4$  in. black polished Carrera plate. This was covered with an  $8 \times 2 \times 1/8$  in. clear Lucite top plate separated from the bottom black plate by a spacer of 0.025-cm Mylar® film cut out in the shape of a model channel. Mobile phase was supplied to the channel with a Model 100-A metering pump (Altex Scientific, Berkeley, CA, U.S.A.). Samples were introduced with a Model CV-6-VHPa-N-60 microsampling valve (Valco Instruments, Houston, TX, U.S.A.), using a 50- $\mu$ l loop. A sample of Dow polystyrene latex standards (Dow Diagnostics, Dow Chem., Midland, MI, U.S.A.) consisting of 1.0% of each 0.20- and 0.481- $\mu$ m particles was used to study flow characteristics of this channel.

Fig. 1 contains pictures that were taken of the sample-particle injection patterns obtained at a mobile phase flow-rate of 0.5 ml/min. Samples were introduced into the channel at zero force field from the sample loop via  $57 \times 0.046$  cm I.D. (0.160 cm O.D.) stainless-steel tubing. Fig. 1A shows that the sample was initially introduced at the channel inlet in a relatively circular pulse. Figs. 1B–D obtained successively after injection show that the sample-inlet profile assumes a parabolic shape under the zero-force-field conditions, probably because of the 90° inlet configuration used. Figs. 1B–D also show that the particles exhibit some streaming irregularities (*e.g.*, arrow in Fig. 1C), presumably because of irregularities in the ends of the tube introducing the sample. Fig. 1E shows that by the time the peak reached the outlet of this short channel (not shown; on the right in these figures), sample particles still were streaming out of the inlet tube (*e.g.*, see arrow).

Fig. 2 shows similar flow patterns in this model channel, obtained under other

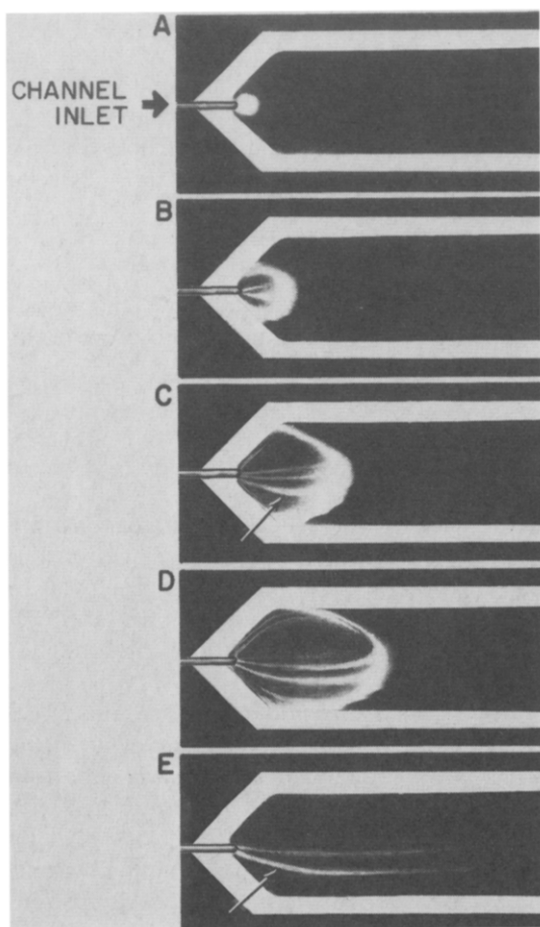


Fig. 1. Inlet flow patterns —valve-loop injection. Transparent channel, 6 in.; loop injection, 50  $\mu$ l of 1% each of 0.220 and 0.481  $\mu$ m polystyrene latices flow-rate, 0.50 ml/min. A-D, Shape of particle band with passing time. E, Inlet, showing particle “streaming”.

operating conditions. Figs. 2A and B show effects on sample band at the channel inlet as a function of flow-rate. Apparently, flow irregularities are decreased at a lower flow-rate (e.g., 0.2 ml/min; Fig. 2B). In Fig. 2C an injection was made in which the original inlet tube was removed and a small sample was injected directly into the inlet of the channel with a syringe. The tube was then replaced and flow initiated in the same manner as in Fig. 2A. Results were essentially the same as for the loop injection in Fig. 2A. Figs. 2D and E show the shape of the particle sample band as it approaches the outlet of the channel tube. The original parabolic flow profile is maintained throughout elution.

The same 6 in. model channel was used to study the effect of injecting the sample, not at the channel inlet, but at a point beyond the inlet just when the full width of the channel is realized. This technique is called center-point injection. Fig. 3 shows the pattern of particle bands obtained with the technique in a 0.0125 cm thick channel. Fig. 3A shows that syringe injection of the sample with no mobile

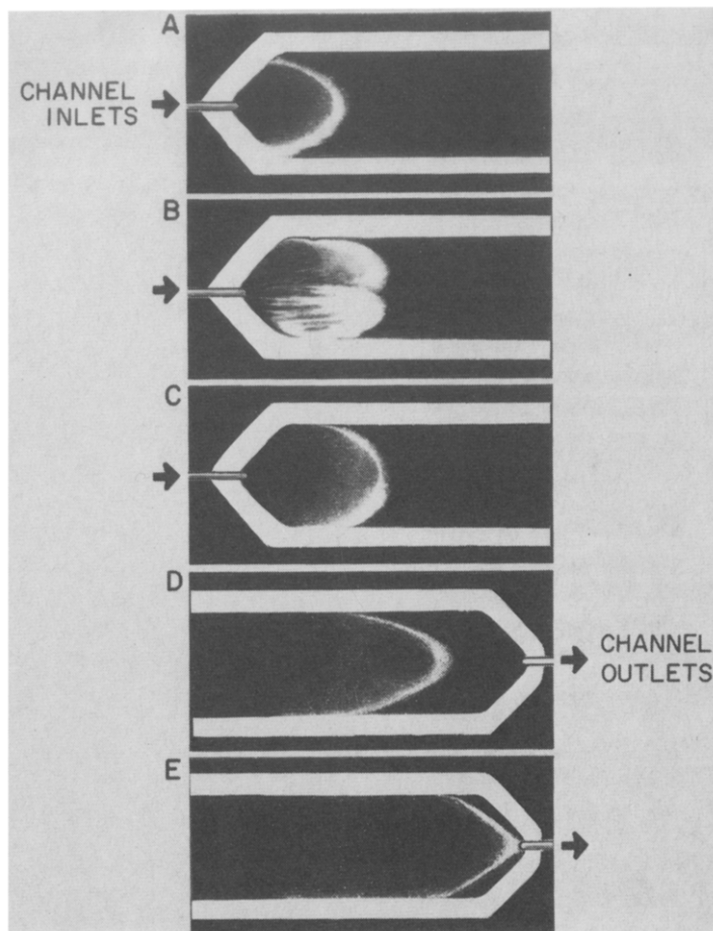


Fig. 2. Effect of flow-rate on particle band shape. A, Loop injection, flow-rate = 0.50 ml/min; B, loop injection, flow-rate = 0.20 ml/min; C, syringe injection, flow-rate = 0.50 ml/min; D and E, same as C, but pattern at outlet. Other conditions as in Fig. 1.

phase flow produces a circular particle pattern at the point of introduction. In Fig. 3B, at a low flow-rate (0.5 ml/min) the original sample spot moves down the channel with essentially no change in size, as might be predicted for the extremely slow diffusion of particles in liquids. In effect, the channel operates as an "infinite-width" system. In Figs. 3C and D, a higher flow-rate (2.0 ml/min) causes the sample pulse to move similarly down the channel (Fig. 3D is at a later time than 3C). Fig. 3E shows a similar sample pattern for a 10- $\mu$ l injection of 1% of 0.481- $\mu$ m polystyrene latex.

In all cases illustrated in Fig. 3, the particulate samples left a "trail" from the inlet to the outlet of the channel, presumably due to the fact that some of the particles are caught up in the "dead" regions of the laminar flow next to the channel wall. Patterns similar to that in Fig. 3E were also found when 10- $\mu$ l portions of 5% of 2000 Å silica sol were injected.

The plates in Fig. 4 illustrate the outflow of particle samples in the manner

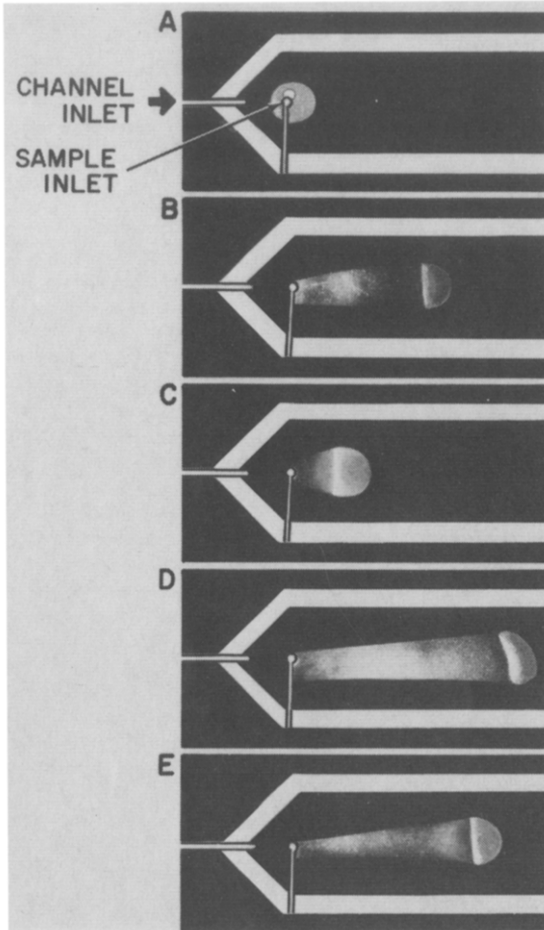


Fig. 3. Inlet flow patterns—center-point injection. A and B, flow-rate, 0.50 ml/min; C and D, flow-rate, 2.0 ml/min; E, 0.481  $\mu\text{m}$  polystyrene particles only, flow-rate 0.50 ml/min. Other conditions as in Fig. 1.

described for Fig. 3. Figs. 4A and B made with a flow-rate of 2.0 ml/min show the particle sample "pulse" just before arriving at the outlet, and arriving at the outlet, respectively. In Fig. 4A the main pulse "a" and the trailing particles "b" can be seen clearly. Figs. 4C-4E show the sample pulse at a flow-rate of 0.5 ml/min as it approached and eluted from the outlet. The asymmetry of the particle profiles in Fig. 4 is believed to be caused by thickness irregularities in the model channel.

These studies suggest that introduction of the sample at a "V-shaped" 90° inlet results in a distorted sample-band front, and that the sample band from such injection occupies the entire span of the channel. On the other hand, center-point injection downstream from the inlet in the center of the channel produces a sample band that moves directly down the center of the channel and only occupies the space within the channel taken up by the original injection volume—the sample does not occupy the entire span of the channel. In all cases "trailing" of sample particles was seen within the channel regardless of the method of sample introduction.

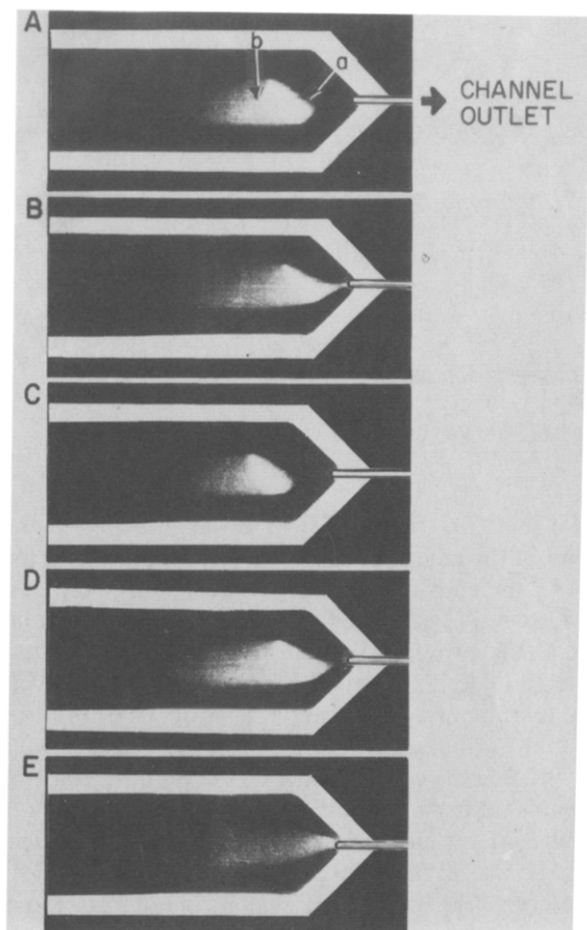


Fig. 4. Outlet flow patterns —center-point injection. A and B, flow-rate, 2.0 ml/min; C-E, flow-rate, 0.50 ml/min. Other conditions as in Fig. 3.

#### *Particulate patterns from sample injection*

A second set of experiments involved the use of a stationary model channel whose dimensions were a close duplicate of those of the rotating channels in our SFFF instruments<sup>2,4</sup>. Special lighting and photographic techniques were developed to visualize the flow patterns of polystyrene latex and India ink samples within the channel in a variety of sampling and flow conditions.

As illustrated schematically in Fig. 5, the model channel was constructed from two sheets of Plexiglas of  $5.1 \times 45.7 \times 0.32$  cm. A 0.025-cm vinyl spacer formed the one-inch-wide channel between the Plexiglas sheets (diagonally-hatched area "a", Fig. 5). The model channel was held together as a sandwich with twenty-two No. 50 binder clips (IDL, Carlstadt, NJ, U.S.A.) distributed evenly around the perimeter of the assembly ("b", Fig. 5). PTFE tubing (0.081 cm I.D., 0.159 cm O.D.) was press-fitted into holes ("c" and "d", Fig. 5) in the Plexiglas top-piece at the apices of the 90° angles at the inlet and outlet of the channel. The tubing ends were made flush

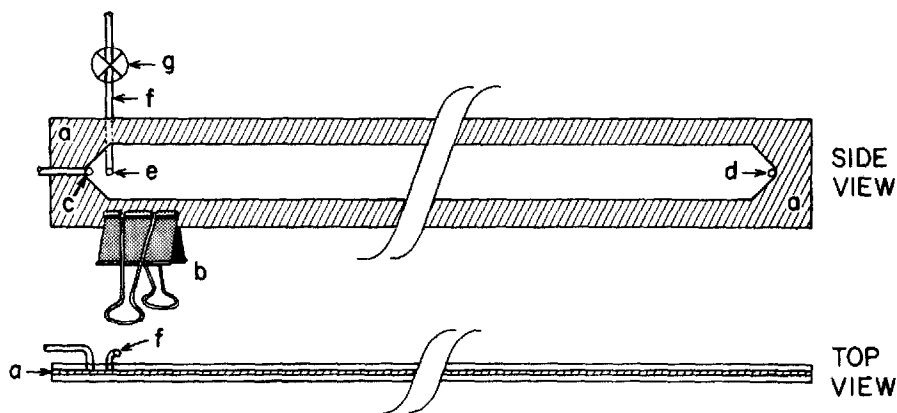


Fig. 5. Schematic of full-length transparent channel. Key to a-g given in text.

with the inner surface of the plastic sheet. A third PTFE tube was attached in the same manner in the center of the end of the channel (hole "e", Fig. 5), even with the apices of the obtuse angles formed by the ends of the channel. This additional inlet simulated a center-point-injection system. A bead of epoxy glue was placed around each tube-hole junction to provide a leak-proof seal.

During these tests the 45.7-cm longitudinal axis of the channel (Fig. 5) was situated horizontally and the 5.1-cm transverse axis was in a vertical position, to duplicate the ambient (1 g) force that normally acts on the transverse axis of our SFFF apparatus. A guide tubing ("f", Fig. 5) was attached to the point-injector of the channel and curved upward. To this tubing was attached a PTFE ball-valve ("g", Fig. 5) that was rigidly clamped. This configuration held the guide tubing in a vertical position similar to that employed in an actual SFFF apparatus. Valve "g" in Fig. 5 and the outlet tubing from the detector were established at the same height above the channel to provide a uniform head of liquid mobile phase.

To make a center-point injection, the pump was turned off and valve "g" was opened. A length of polyethylene tubing (0.025 cm I.D.  $\times$  0.061 cm O.D.), attached to a 25- $\mu$ l microsyringe was then fed through the valve and the tubing into the channel inlet. A small piece of Plasticine was packed around the polyethylene to form a liquid-tight seal with the valve.

For these tests a Model 850 metering pump (DuPont Biomedical Products Department, Wilmington, DE, U.S.A.) was used to supply the mobile phase, which then passed through a Model AHCV-6-UHPa-N60 sampling valve (Valco) connected to inlet tube "c" (Fig. 5). The outlet tubing "d" from the channel was connected to a DuPont Model 901 UV spectrophotometer. This arrangement allowed the peak being observed visually also to be subsequently detected turbidimetrically and plotted by the recorder.

Photographic documentation of the particle-flow patterns within this channel was carried out by macroscopic dark-field illumination<sup>9</sup>. The model channel was placed 35 cm in front of a black velvet backdrop and illuminated obliquely from behind by two collimated light sources. This method of illumination rendered everything in the field of view black, except the particulate sample which "radiated" white



light due to scattering. (Under normal lighting conditions samples of this nature are virtually transparent.) Photography was carried out with a Model OM-2n 35-mm camera body (Olympus Camera, Woodbury, NY, U.S.A.) mounted to a Series-1 70–210 mm zoom lens (Vivitar, Santa Monica, CA, U.S.A.) operated in the close-focusing mode and situated 100 cm from the model channel. To the front of the lens was mounted a bellows with a horizontal slit-mask to reduce reflection by stray light. Exposures were 0.5 sec at  $f$  5.6 on Tri-X pan film (Eastman-Kodak, Rochester, NY, U.S.A.) rated at an exposure index of 800. The 0.5-sec exposures used to photograph the flow patterns required that the mobile phase flow be interrupted during the exposure. This technique caused no visible artifacts.

Fig. 6A shows the pattern that was obtained when a 25- $\mu$ l sample of 1% of 0.176- $\mu$ m polystyrene latex standard was injected from the valve loop at 0.5 ml/min. (This is a technique similar to that often used in actual SFFF separations.) The bullet-shaped profile of the band in Fig. 6A is probably caused by uneven flow characteristics at the inlet of the channel, for the same reasons given for Figs. 1 and 2. The streaking of particles which extends from the particle-front back to the inlet is likely caused by uneven flow characteristics inside the inlet tubing and/or the point at which the tubing enters the channel. Fig. 6B shows the same sample as in Fig. 6A after the flow has been interrupted for 1.0 min, simulating a 1-min relaxation or equilibration. Note that the profiles in Figs. 6A and 6B are virtually identical, suggesting that an interruption of flow has no significant effect on the profile of the particle. Figs. 6C–E show the particle band as it travels down the channel at a flow-rate of 2.0 ml/min. The streaking of the particle band is still evident; however, the band front appears to be somewhat flatter. While the profile in Figs. 6C–E suggests that the velocity of mobile phase is greater at the edges of the channel than in the center, this effect may be the result of an artifact caused by uneven thickness of this model channel.

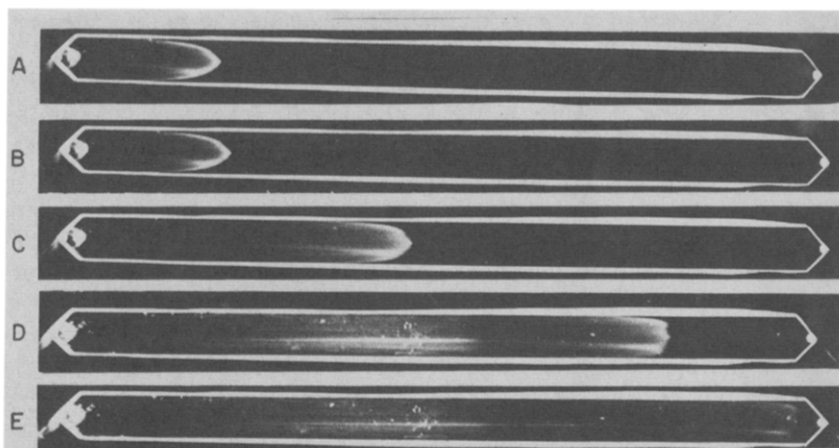


Fig. 6. Particle band patterns in full-length channel —valve-loop injection. Channel, 43 cm; sample, 25  $\mu$ l of 0.176- $\mu$ m polystyrene latex. A, Flow-rate, 0.50 ml/min; B, same as A with flow interruption of 1.0 min; C–E, flow-rate, 2.0 ml/min.

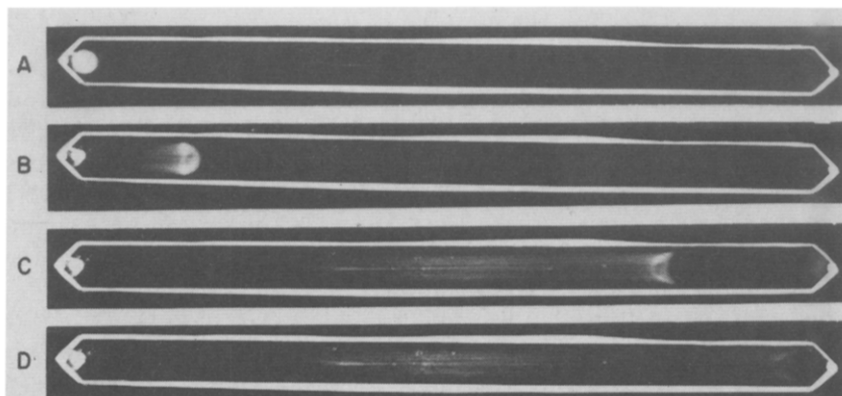


Fig. 7. Particle band patterns in full-length channel—center-point injection. A, Injection, no flow; B–D, flow-rate, 2.0 ml/min. Other conditions as in Fig. 6.

Results of center-point injection are summarized in Fig. 7. Fig. 7A shows the pattern of a 25- $\mu\text{l}$  injection of the polystyrene latex standard in which the sample was deposited as a pulse (disc) in the center of the channel inlet. Figs. 7B–D show the particles travelling down the center of the channel after a 2.0 ml/min flow-rate was imposed. Note that the particles do not touch the sides of the channel during travel, as does the more highly dispersed valve-injected sample illustrated in Fig. 6. However, an apparent faster velocity near the edge of the channel (channel imperfection?) converts what began as a convex sample front at the channel inlet into a concave shape by the time the peak has traversed about two-thirds of the channel. As might be predicted by these flow patterns, the center-point injection technique causes less band spreading and consequently, sharper peaks than those from valve injection. However, the sharpening of band shape by center-point injection is not significant, as illustrated by the elution fractrograms in Fig. 8.

Attempts to analyze large particles (*ca.* 0.5  $\mu\text{m}$ ) in an SFFF apparatus in which the channel thickness is perpendicular to the earth's gravity (channel span parallel with the earth's gravity) can result in anomalies relating to the peak-shape profile. Fig. 9 shows the results of the valve-injection of a 0.481- $\mu\text{m}$  polystyrene latex (0.5% solids). Fig. 9A shows the particles after being injected at 0.5 ml/min for 1.0 min. Figs. 9B and C depict the particles at various stages after travelling down the channel at 2.0 ml/min. Note that the lower part of the particle front has been distorted outward from the normal symmetrical "bullet"-shape found for smaller particles (Figs. 1 and 2).

Even more striking are the results in Fig. 10 which show the large-particle (0.481  $\mu\text{m}$ ) sample after slow valve injection at 0.06 ml/min for 8.3 min (same volume of injection as for Fig. 9 but at a slower rate and longer time). In Fig. 10 the large particles are sufficiently affected by ambient gravity to settle towards one edge of the channel (at the bottom in the photo) during the slow injection process. Figs 10A–E show the travel of these particles down the channel at 2.0 ml/min following injection. In this case most of the sample particles actually sink to the bottom of the channel,

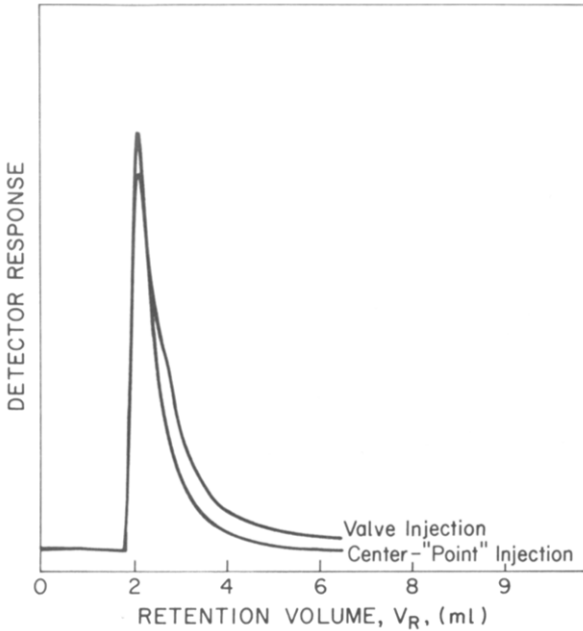


Fig. 8. Elution pattern: valve-loop vs. center-point injection. Unretained 0.176- $\mu$ m polystyrene latex; flow-rate, 0.5 ml/min.

thus occupying only a portion of the channel span, one-third to one-half of the span in the case of Fig. 10C. When Fig. 10E is compared with Fig. 10C it is evident that the sample stretches from the channel outlet back almost to the inlet.

With the different flow-rates used in Figs. 9 and 10, the same clearing volume from the channel occurs, with comparable eluting band widths. This observation is in keeping with other findings that, for a given channel length and for comparable operating conditions, channels with a 1.91-cm span produce bands that are approximately equal in band width to channels with a 2.54-cm span.

Studies carried out with India ink produced results which were very close to

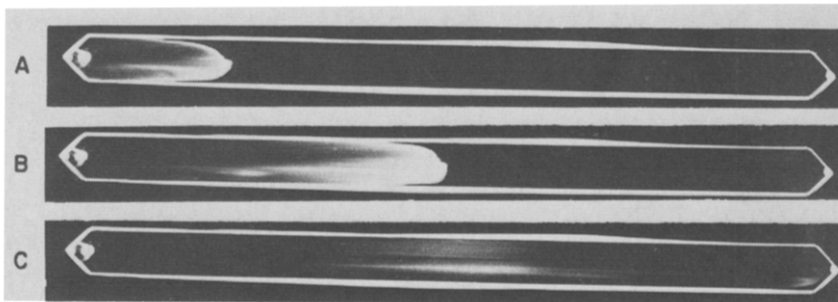


Fig. 9. Valve-loop injection —0.481- $\mu$ m polystyrene latex. A, 25- $\mu$ l Injection for 1.0 min at 0.50 ml/min; C, flow-rate, 2.0 ml/min. Other conditions as in Fig. 6.

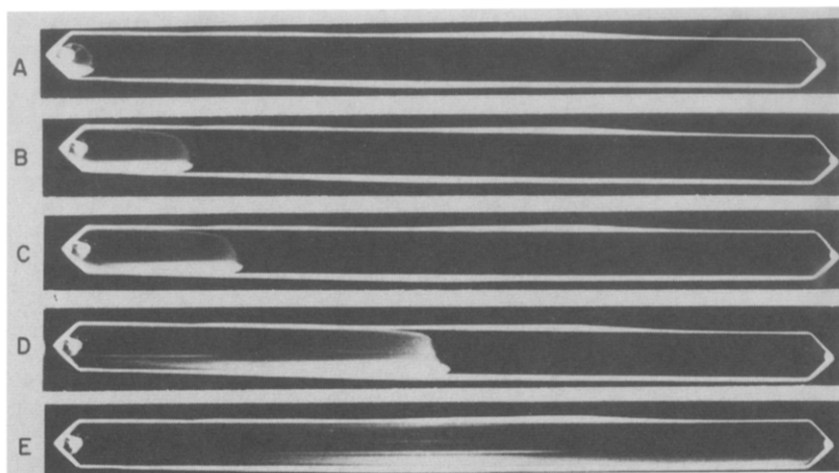


Fig. 10. Very slow valve-loop injection —0.481- $\mu\text{m}$  polystyrene latex. A, 25- $\mu\text{l}$  injection for 8.3 min at 0.06 ml/min; B-E, flow-rate, 2.0 ml/min.

those found for the 0.481- $\mu\text{m}$  polystyrene latex in Figs. 9 and 10. Table I shows that India ink and polystyrene latex exhibit identical retention volumes typical of “break-through” peaks. As previously discussed<sup>4</sup>, “break-through” peaks are due to slow-diffusing particles that move down the middle of the channel at the highest mobile-phase velocity  $U_{\text{max}}$  in the laminar velocity profile. This situation contrasts to that for smaller, faster-diffusing molecules (*e.g.*, acetone) that engage all velocities within the channel. Small molecules elute at a time representative of that for the average mobile phase velocity  $U_0$  to produce a peak at retention volume  $V_0$ . The data in Table I also illustrate that fountain pen ink (Parker’s) exhibits behavior similar to acetone, *e.g.*, retention is not affected by the external force field. The difference in channel plate number values  $N$  for acetone and Parker’s ink cannot be explained.

TABLE I

SAMPLING EFFECTS: RETENTION VOLUME AND CHANNEL PLATE NUMBERS

Condition (sample volume 10 $\mu\text{l}$ )	Retention volume*, $V_R$ (ml)	Channel plate number, $N$
<i>Valve</i>		
Parker’s Ink	3.05	92
Acetone	3.03	209
Polystyrene latex, 0.176 $\mu\text{m}$	2.05**	—
2% India Ink	2.07	—
<i>Center-point injection</i>		
Acetone	2.87**	230
Polystyrene latex, 0.176 $\mu\text{m}$	2.05**	—

\*  $V_R$ , Absolute values, corrected for volumes of inlet and outlet tubing.

\*\* Average of duplicate runs.

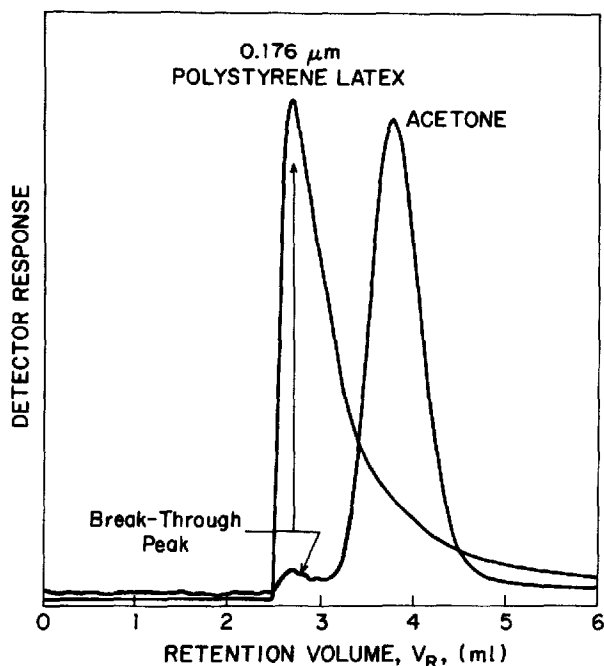


Fig. 11. "Break-through" and  $V_0$  peaks. No force field or relaxation; flow-rate, 0.50 ml/min.

Fig. 11 shows the peak for acetone and the "break-through" pre-peak superimposed on the 0.176- $\mu\text{m}$  polystyrene latex peak. This fractogram clearly shows the relationship between "break-through" peaks and components that are totally unretained in an SFFF channel.

It may be concluded from these studies that center-point injection results in less band broadening for the injected sample, relative to the volume associated with particles injected with the incoming mobile phase stream (e.g., valve-loop injection). Center-point-injection techniques in SFFF are somewhat analogous to those in high-performance liquid chromatography (HPLC) wherein the particles travel down the center of the channel and never reach the wall of the channel span. In effect then, center-point injection in SFFF is analogous to the "infinite-diameter" columns in HPLC. These studies have demonstrated that the model channel is a good indicator of primary flow characteristic inside a working SFFF channel. However, conclusions formed from results with the model channel need to be tempered with the realization that the movement of particles can be significantly different within a channel with an imposed force field. The model channel with no imposed external force field merely provides basic information on the flow characteristics of unretained components.

#### *Sampling procedures*

It was observed that the manner in which the sample is injected into an SFFF channel can significantly affect the results of particle-size or particle-mass calculations. Therefore, a systematic study of sampling effects was carried out using constant force-field conditions with a 0.176- $\mu\text{m}$  nominal size polystyrene latex standard. Table

TABLE II

## EFFECT OF SAMPLING CONDITIONS; VALVE-LOOP INJECTION AT CONSTANT FORCE FIELD

Conditions: 0.022-cm "floating" channel, 2.54-cm span, mobile phase, 0.1% Aerosol-OT, except as noted; polystyrene latex standard, 0.176  $\mu\text{m}$  diameter (nominal); calculated particle size corrected for steric effect.

Run designation	Rotor speed (rpm)	Sample volume ( $\mu\text{l}$ )	Sample concentration (wt. %)	Relaxation time (min)	Flow-rate (ml/min)	Sample loop sweep for injection	Calculated mean particle diameter ( $\mu\text{m}$ )	Remarks
AV	6000	25	0.10	10.0	4.0	1.0 min at 0.5 ml/min	0.158	
AY	6000	10	0.05	10.0	4.0	1.0 min at 0.5 ml/min	0.159	
BA	6000	25	0.10	10.0	1.0	1.0 min at 0.5 ml/min	0.159	
BK	6000	25	0.10	10.0	4.0	1.0 min at 0.5 ml/min	0.158	
BV	6000	10	0.10	10.0	4.0	1.0 min at 0.5 ml/min	0.159	
BW	6000	10	0.10	10.0	4.0	1.0 min at 0.5 ml/min	0.159	Channel inlet and outlets reversed
BX	6000	10	0.10	10.0	4.0	1.0 min at 0.5 ml/min	0.161	Mobile phase, 0.25% Aerosol-OT
BB	6000	25	0.10	10.0	4.0	1.0 min at 0.5 ml/min	0.154	Mobile phase density, 1.46 with glycerine
BC	6000	25	0.10	10.0	4.0	1.0 min at 0.5 ml/min	0.153	Mobile phase, 0.1% FL-70
BG	4000	25	0.10	10.0	4.0	1.0 min at 0.5 ml/min	0.158	
BJ	2000	25	0.10	10.0	4.0	1.0 min at 0.5 ml/min	0.164	
BL	2000	25	0.10	30.0	0.50	1.0 min at 0.5 ml/min	0.162	
BM	1000	25	0.10	30.0	0.10	1.0 min at 0.5 ml/min	0.156	
AW	6000	25	0.10	5.0	4.0	8.3 min at 0.06 ml/min	0.161	
CM	2060	10	0.10	10.0	4.0	8.3 min at 0.06 ml/min	0.172	
CN	2060	10	0.10	10.0	4.0	4.2 min at 0.06 ml/min	0.178	
AX	6000	25	0.10	5.0	4.0	Repeat AW; injection at 10,000 rpm, run at 6000 rpm	0.159	
BD	6000	25	0.10	10.0	4.0	0.5 min at 0.5 ml/min	0.159	100- $\mu\text{l}$ PTFE tubing loop; inject 25 $\mu\text{l}$ from loop only
BR	6000	1	2.5	10.0	4.0	8.3 min at 0.06 ml/min	0.153	
BS	6000	10	0.10	10.0	4.0	0.5 min at 0.50 ml/min	0.165	"Bolus" sampling with sweep of 20% larger volume than connecting tube
BT	6000	10	0.10	10.0	4.0	0.5 min at 0.50 ml/min	0.163	Repeat BS with 35% larger sweep volume

II summarizes the results obtained during this study in which a wide variety of sampling conditions was used.

No significant change in apparent particle diameter occurs with modest changes in sample volume or concentration. Runs AV-BV showed essentially no difference in the calculated mean particle diameter for the polystyrene latex standard measured at a rotor speed of 6,000 rpm at sample volumes of 10 or 25  $\mu\text{l}$  and sample concentrations of 0.05 and 0.10%. (In these experiments the samples were injected with the incoming mobile phase stream for 1.0 min at a flow-rate of 0.5 ml/min. The flow was then interrupted and the sample relaxed for 10.0 min at the 6000 rpm running speed.) Also, no difference in particle diameter was observed when the mobile phase flow-rate was 1.0 or 4.0 ml/min. It should be noted that the calculated mean particle diameter of approximately 0.159  $\mu\text{m}$  for these experiments is smaller than the manufacturer's specified diameter of 0.176  $\mu\text{m}$ . This discrepancy is discussed in another publication<sup>10</sup>.

No change in the calculated particle diameter was found when the inlet and outlet tubings of the channel were reversed during the separation so the direction of the flow was changed relative to the rotation during the separation process (Run BW). Only small changes in the calculated particle diameter were noted when the concentration of Aerosol-OT dispersant was increased to 0.25% from the usual 0.1% (Run BX), or when the mobile phase density was increased to 1.146 by the addition of glycerine. (Run BB), or when an entirely different (cationic rather than anionic) dispersant was used (*e.g.*, 0.1% FL-70) (Run BC). Apparently, these substantial changes in the type and concentration of dispersant and the density of the mobile phase into which the sample was introduced perturbed the retention process very little for this method of sample introduction.

Use of lower rotor speeds during both injection retention and subsequent fractionation (Runs BG and BJ) resulted in only small changes in the calculated particle diameter. Increasing the relaxation time from 10 min to 30 min (Run BL) also shows no significant effect, even at a very low mobile phase flow-rate (0.50 ml/min). The calculated particle diameter is essentially unchanged with further decrease in rotor speed (Run BM) with a very low mobile phase flow-rate (0.10 ml/min) for this method of sample introduction.

Sweeping the contents of the sampling valve loop at a very low flow-rate (same total sweeping volume) had little effect on the calculated particle diameter (Run AW). However, increasing the concentration of the particles with this sampling technique slightly decreased the calculated particle diameter (Run BR). This effect is commonly observed when too high a sample concentration of small particles is injected into an SFFF channel. Charged particles at higher concentrations, when forced near the wall, interfere with each other so that their normal distance from the wall ( $\ell$  value) is not reached. In this state the charged particles repel each other and equilibrate at a distance from the wall slightly farther than theoretical. These repelling particles then are intercepted by higher-velocity flow streams and elute early, producing smaller particle-diameter values than theory predicts.

Introducing the sample from a PTFE sample loop that is only partially filled with the sample by syringe showed no significant effects on particle-diameter measurement (Run BD). However, introducing an air bubble at both ends of the sample in the loop so that the sample is segmented from the flowing liquid to the channel

TABLE III  
EFFECT OF OPERATING CONDITIONS

Conditions: same as for Table II, except polystyrene standards as indicated; corrected for steric effect; relaxation time, 10.0 min; flow-rate, 4.0 ml/min.

<i>Run designation</i>	<i>Rotor speed (rpm)</i>	<i>Sample volume (<math>\mu</math>l)</i>	<i>Sample concentration (wt. %)</i>	<i>Sample loop sweep for injection</i>	<i>Manufacturer's nominal particle diameter (<math>\mu</math>m)</i>	<i>Calculated mean particle diameter (<math>\mu</math>m)</i>	<i>Remarks</i>
BH	6000	25	0.1	1.0 min at 0.5 ml/min	0.085	0.069	
BQ	15,000	10	0.2	1.0 min at 0.5 ml/min	0.085	0.064	
AZ	6000	25	0.05	1.0 min at 0.5 ml/min	0.220	0.205	
BI	2000	25	0.04	1.0 min at 0.5 ml/min	0.312	0.301	
BN	2000	10	0.05	5.0 min at 0.1 ml/min	0.497	0.426	100- $\mu$ l PTFE tubing loop; inject 10 $\mu$ l from loop only
BO	1000	10	0.05	5.0 min at 0.1 ml/min	0.497	0.430	100- $\mu$ l PTFE tubing loop; inject 10 $\mu$ l from loop only
BP	1000	1	10.0	5.0 min at 0.1 ml/min	0.497	0.433	100- $\mu$ l PTFE tubing loop; inject 10 $\mu$ l from loop only



("bolus" flow) does produce a small but significant effect (Runs BS and BT). It appears that this special "bolus" flow sampling technique is the most precise in placing a sample onto the channel with a minimum of particle-band perturbation.

The effect of sampling with varying constant forcefield conditions is shown in Table III. Little difference in the calculated mean particle diameter was found for a nominal 0.085- $\mu\text{m}$  polystyrene latex fractionated at 6000 or 15,000 rpm with changes in sample volume and particle concentration, using a 1 min sample-loop sweep time at a flow-rate of 0.5 ml/min. (Runs BH, BQ). Similar results were obtained with larger-diameter polystyrene latex standards (Runs AZ, BI). No significant effects on calculated particle diameter were noted with the largest nominal particle size (0.497  $\mu\text{m}$ ) even when high concentrations (10 wt. %) and very small sample volumes (10  $\mu\text{l}$ ) were injected into a 100  $\mu\text{l}$  PTFE sampling valve loop (Runs BN, BO, BP).

Since the preliminary results given in Table II indicated that "bolus" flow injection technique may provide a means for the best sample injection in SFFF, a more detailed study of this approach was carried out. Table IV lists the results of these and other experiments.

A number of interesting conclusions may be drawn from the studies shown in Tables II-IV. For example, the data suggest that sweeping the particulate sample from a completely filled loop at a very slow flow-rate results in a somewhat higher calculated particle diameter relative to the same sample sweep-out at a higher flow-rate with the same sweep volume (but in a shorter time). This trend suggests that sweeping the sample out of the sample loop into the channel via the mobile phase inlet at higher flow-rates causes the sample to be convectively mixed with the mobile phase so that it occupies a larger channel volume and effectively moving the sample further down the channel during the sampling process. This effect results in early elution and a smaller calculated particle size. Thus, it appears that more accurate particle size or mass measurements are carried out when the sample is placed in the channel very slowly with a minimum of mixing with the mobile phase in the channel. Sampling apparently is largely unaffected by relaxation time as long as it is sufficient for the particular separation in question. Retention and the calculated particle diameter also are unaffected over relatively wide changes in the flow-rate with which the separation is conducted.

The results in Table IV also show that for small particles the observed particle diameter is a function of the force field under which the relaxation and separation are carried out. At lower force fields the smaller particles tend to move down the channel during sampling. In general, the higher the force field, the more likely is the correct retention. While retention appears to be generally more accurate when "bolus" flow injection is employed, this technique is impractical. Unfortunately, it has the disadvantage of leaving air bubbles in the channel that can complicate detection.

The data in Table IV also show that reducing the channel span from 2.54 to 1.91 cm has no appreciable effect on retention, providing mobile phase velocity and other parameters are maintained, relative to the channel-span change. As might be expected, the lower-volume channel appears more susceptible to overloading by larger sample volumes and higher sample concentrations. Retention with reverse-channel flow is again identical with the narrow-span channel.

Data in Tables II-IV further suggest that the diameter of polystyrene latex standards may be different from the manufacturer's reported value. In fact, previous

TABLE IV  
 COMPARISON OF "BOLUS" FLOW AND FILLED-LOOP INJECTION TECHNIQUES WITH CONSTANT FORCE FIELD  
 Sample injection technique A, standard filled-loop injection; B, "Bolus" flow injection.

Run designation	Rotor speed (rpm)	Sample volume ( $\mu$ l)	Sample concentration (wt. %)	Relaxation time (min)	Flow-rate (ml/min)	Sample loop sweep for injection	Sample injection technique	Channel span (cm)	Manufacturer's nominal particle diameter ( $\mu$ m)	Calculated mean particle diameter ( $\mu$ m)	Remarks
BY	2070	10	0.1	10.0	4.0	0.61 min at 0.5 ml/min	B	2.54	0.176	0.181	
BZ	1530	10	0.1	10.0	1.0	0.61 min at 0.5 ml/min	B	2.54	0.176	0.171	
CM	2060	10	0.1	10.0	4.0	8.3 min at 0.06 ml/min	A	2.54	0.176	0.172	
CN	2060	10	0.1	10.0	4.0	4.2 min at 0.06 ml/min	A	2.54	0.176	0.178	
CH	15,000	10	0.1	10.0	4.0	1.0 min at 0.5 ml/min	A	2.54	0.091	0.072	
CI	15,000	10	0.1	10.0	4.0	8.3 min at 0.06 ml/min	A	2.54	0.091	0.078	
CJ	10,000	10	0.1	10.0	4.0	8.3 min at 0.06 ml/min	A	2.54	0.091	0.079	
CA	15,000	10	0.2	10.0	4.0	0.61 min at 0.5 ml/min	A	2.54	0.085	0.057	
CB	15,000	25	0.2	10.0	4.0	0.61 min at 0.5 ml/min	A	2.54	0.085	0.062	
CC	15,000	10	0.5	10.0	4.0	0.61 min at 0.5 ml/min	B	2.54	0.085	0.064	
CD	15,000	10	0.5	10.0	4.0	8.3 min at 0.06 ml/min	A	2.54	0.085	0.064	
CE	15,000	10	0.1	10.0	4.0	0.61 min at 0.5 ml/min	B	2.54	0.085	0.061	
CF	15,000	10	0.1	10.0	4.0	8.3 min at 0.06 ml/min	A	2.54	0.085	0.066	
CG	15,000	10	0.1	10.0	1.0	8.3 min at 0.06 ml/min	A	2.54	0.085	0.067	

CK	20,000	10	0.1	10.0	4.0	8.3 min at 0.06 ml/min	A	2.54	0.085	0.070	Repeat CP Reversed channel flow
CL	20,000	10	0.5	10.0	4.0	8.3 min at 0.06 ml/min	A	2.54	0.085	0.063	
CO	15,000	10	0.5	30.0	4.0	8.3 min at 0.06 ml/min	A	2.54	0.085	0.062	Repeat CP Reversed channel flow
CP	15,000	10	0.5	10.0	4.0	4.2 min at 0.06 ml/min	A	2.54	0.085	0.069	
CQ	15,000	10	0.5	10.0	4.0	4.2 min at 0.06 ml/min	A	2.54	0.085	0.068	Repeat CP Reversed channel flow
CR	15,000	10	0.5	10.0	4.0	8.3 min at 0.06 ml/min	A	2.54	0.085	0.065	
CS	15,000	10	0.5	10.0	4.0	4.2 min at 0.06 ml/min	A	2.54	0.085	0.069	Repeat CP Reversed channel flow
CT	20,000	10	0.5	10.0	4.0	8.3 min at 0.06 ml/min	A	2.54	0.085	0.068	
CU	20,000	10	0.5	10.0	4.0	4.2 min at 0.06 ml/min	A	2.54	0.085	0.068	Repeat CP Reversed channel flow
CV	20,000	10	0.5	10.0	4.0	8.3 min at 0.06 ml/min	A	2.54	0.085	0.068	
CW	6080	10	0.1	10.0	3.0	4.2 min at 0.06 ml/min	A	1.91	0.176	0.154	Repeat CP Reversed channel flow
CX	2070	10	0.1	10.0	3.0	4.2 min at 0.06 ml/min	A	1.91	0.176	0.176	
CY	3040	10	0.1	10.0	3.0	4.2 min at 0.06 ml/min	A	1.91	0.176	0.166	Repeat CP Reversed channel flow
CZ	20,000	10	0.5	10.0	3.0	4.2 min at 0.06 ml/min	A	1.91	0.085	0.061	
DA	15,000	10	0.5	10.0	3.0	4.2 min at 0.06 ml/min	A	1.91	0.085	0.061	Repeat CP Reversed channel flow
DB	20,000	10	0.5	0	3.0	4.2 min at 0.06 ml/min	A	1.91	0.085	0.061	
DC	20,000	10	0.5	0	3.0	8.3 min at 0.06 ml/min	A	1.91	0.085	0.061	Repeat CP Reversed channel flow
DD	20,000	10	0.5	0	3.0	8.3 min at 0.06 ml/min	A	1.91	0.085	0.058	
DE	20,000	10	0.5	0	3.0	4.2 min at 0.06 ml/min	A	1.91	0.085	0.060	Repeat of DD Reversed channel flow
DF	20,000	10	0.5	0	3.0	8.3 min at 0.06 ml/min	A	1.91	0.085	0.058	
DG	20,000	10	0.5	0	3.0	5.0 min at 0.10 ml/min	A	1.91	0.085	0.059	

TABLE V

NOMINAL vs. MEASURED PARTICLE DIAMETERS FOR POLYSTYRENE LATEX STANDARDS

Particle diameter in  $\mu\text{m}$ .

Manufacturer's value*	Measured value**	Difference	
		$\mu\text{m}$	%
0.085	0.067 $\pm$ 0.005	+0.018	+21
0.091	0.081 $\pm$ 0.004	+0.010	+11
0.176	0.163 $\pm$ 0.006	+0.013	+7
0.220	0.222 $\pm$ 0.010	-0.002	-1
0.312	0.329 $\pm$ 0.020	-0.017	-5
0.481	0.535 $\pm$ 0.012	-0.054	-11

\* Transmission electron microscopy.

\*\* Ref. 10; average of TEM and SFFF measurements from two laboratories.

studies have shown this to be the case, based on continuous force-field and TDE-SFFF measurements, as well as transmission electron microscopic (TEM) analyses<sup>10</sup>. Table V compares the manufacturer's value with the best values obtained by averaging SFFF and TEM measurements carried out in this and other laboratories. Some values check reasonably well, but small particles appear to be significantly smaller and the larger particles appear somewhat larger than reported by the manufacturer.

#### Sampling valve loop-sweeping studies

The manner in which the sample is swept from the sample valve loop into the channel can affect band broadening in SFFF separations. To study this effect a simple apparatus was assembled consisting of a sampling valve with external loop connected to an empty 40  $\times$  0.081 cm I.D. stainless-steel tube with a volume of 0.212 ml. (This arrangement simulates the connecting tube from the valve to the channel used in our actual SFFF equipment.) To this tube was then directly attached a UV photometric detector (254 nm) equipped with a 1- $\mu\text{l}$  cell<sup>11</sup>. The sample, consisting of 0.025% of 0.176- $\mu\text{m}$  polystyrene latex standard, was loaded into the sample valve loop by one of several techniques and swept through the connecting tube into the detector at a 0.1% Aerosol-OT mobile phase flow-rate of 0.50 ml/min. The volume of the resultant peak for the polystyrene latex standard was measured from the beginning to the end of the peak, roughly a 6-sigma interval. Since previous studies (*e.g.*, Figs. 1 and 2) indicated "trailing" of a polystyrene latex from connecting tubes, these peaks were considerably tailing (asymmetry factors<sup>12</sup> greater than 2), making exact volume measurements somewhat imprecise.

Several interesting conclusions can be drawn from the results shown in Fig. 12. Greatest peak broadening generally was found when the stainless-steel sample loop was completely filled with the sample and the entire volume swept into the simulated separating system. Packing the 40-cm connecting tubing with 70- $\mu\text{m}$  glass beads significantly reduced band broadening for all sample loop sizes tested. Presumably, the glass beads break up the normal laminar flow pattern whereby particles tend to be swept very slowly from the walls of the tubing where flow velocity is very

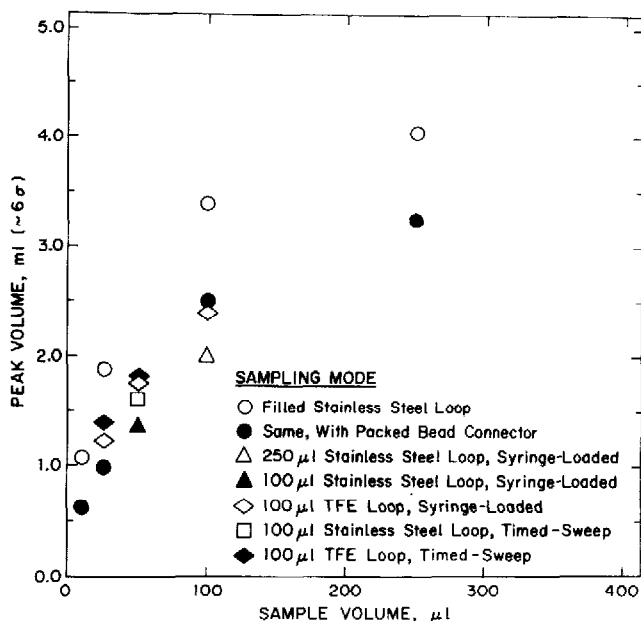


Fig. 12. Effect of valve-loop sampling technique. Sample, 0.025% of 0.176- $\mu\text{m}$  polystyrene latex; flow-rate, 0.5 ml/min; 0.1% Aerosol-OT; no force field or relaxation.

low. The glass beads also reduced the tube volume by about one-half, which also decreased the potential for band broadening.

Decrease in band broadening was noted when a 250- $\mu\text{l}$  stainless-steel loop was syringe-loaded so that a sample of smaller volume was swept out of the exit-end of the loop directly into the simulated separating system. It would appear, therefore, that in this case the normal exponential dilution within this large sample-loop volume is significantly decreased. A similar effect was noted when a 100- $\mu\text{l}$  stainless-steel loop was partially loaded with a syringe. Approximately the same improved results also were obtained by timed-sweeping a partial-volume "plug" of sample from the loop so that the entire contents of the loop were not involved. No significant difference between the stainless-steel and PTFE sample loops was noted.

In summary, least band spreading appears to take place with a "plug" injection of the sample either syringe-loaded in the outlet loop so that the loop contains only a partial volume of sample, or time-swept from the loop as a "plug". Packing the connector tubing from the loop to the channel with 70- $\mu\text{m}$  glass beads also reduces band broadening, presumably by reducing the particle "trailing" effect.

## REFERENCES

- 1 J. C. Giddings, F. J. F. Yang and M. N. Myers, *Anal. Chem.*, 46 (1974) 1917.
- 2 J. J. Kirkland, C. H. Dilks, Jr. and W. W. Yau, *J. Chromatogr.*, 255 (1983) 255; *U.S. Patents* 4,446,014 and 4,446,015.
- 3 J. C. Giddings, M. N. Myers, K. D. Caldwell and S. R. Fisher, *Methods Biochem. Anal.*, 26 (1980) 79.
- 4 J. J. Kirkland, W. W. Yau, W. A. Doerner and J. W. Grant, *Anal. Chem.*, 52 (1980) 1977.
- 5 J. J. Kirkland, S. W. Rementer and W. W. Yau, *Anal. Chem.*, 53 (1981) 1730.

- 6 W. W. Yau and J. J. Kirkland, *Separ. Sci. Technol.*, 16 (1981) 577.
- 7 J. J. Kirkland and W. W. Yau, *U.S. Patent*, 4,285,810, August 25, 1981.
- 8 J. C. Giddings, M. R. Schure, M. N. Myers and G. R. Velez, *Anal. Chem.*, 56 (1984) 2099.
- 9 A. A. Blaker, *Handbook for Scientific Photography*, Freeman, San Francisco, CA, 1977, p. 251.
- 10 J. J. Kirkland and W. W. Yau, *Anal. Chem.*, 56 (1984) 1461.
- 11 J. J. Kirkland, in S. G. Perry (Editor), *Gas Chromatography 1972*, Applied Science Publ., Barking, 1973, p. 39.
- 12 L. R. Snyder and J. J. Kirkland, *Introduction to Modern Liquid Chromatography*, Wiley, New York, 2nd ed., 1979, p. 222.